

Direct Electrolysis of Molten Lunar Regolith for the Production of Oxygen and Metals on the Moon

A.H.C. Sirk^a, D.R. Sadoway^a, L. Sibille^b

^a Department of Materials Science and Engineering, Massachusetts Institute of Technology, Cambridge, Massachusetts 02139, USA

^b ASRC Aerospace Corp. NASA Kennedy Space Center, Florida 32899, USA

The feasibility of producing oxygen by direct electrolysis of molten lunar regolith at 1600 °C was investigated. Oxygen gas at the anode was generated concomitantly with production of iron and silicon at the cathode from the tightly bound oxide mix. Current efficiencies for oxygen evolution from different melt compositions were determined during the course of electrolysis by on-stream analysis of oxygen gas. Scale-up from thin wire (ca. 0.3 cm²) electrodes to plate and disc electrodes (ca. 10 cm²) was achieved.

Introduction

When considering the construction of a lunar base, the high cost (ca. \$10⁵ kg⁻¹) of transporting materials to the surface of the moon is a significant barrier. Therefore in-situ resource utilization will be a key component of any lunar mission. Oxygen gas is a key resource, abundant on earth but absent on the moon, although half the weight of the moon is oxygen in the form of tightly bound oxides. If oxygen gas could be produced on the moon, this would provide a dual benefit. Not only does it no longer need to be transported to the moon for life support, it can also be used as a fuel oxidizer to support transportation of crew and resources more cheaply (ca. \$2×10⁴ kg⁻¹) from lower earth orbit to the surface of the moon. To this end, a stable, robust, lightly manned system is required to produce oxygen from lunar resources.

The concept of molten oxide electrolysis (a.k.a. magma electrolysis) for the production of iron metal from a silicate melt is not new, having first been patented by Aiken in 1906 (1). Currently, this technology is being investigated for the direct electrolysis of molten lunar regolith at 1575 °C to produce oxygen gas and metals on the moon. Direct molten oxide electrolysis for the electrolysis of molten rocks (2) or for the production of non-terrestrial metal resources has been proposed previously (3, 4) and small scale electrolysis of molten lunar simulant has been demonstrated (5). This technology is ideal for lunar engineering as the absence of a supporting electrolyte reduces the payload. If a self heating cell (as is used in the aluminum industry) is developed, this would further reduce the terrestrial resources required, as solidified regolith could act as the containment vessel and the molten electrolyte resistance between the electrodes would provide the heat required through joule heating (I^2R).

More detailed measurements on the effect of melt chemistry and electrode materials as well as a scale up and quantification of the preliminary results is required in order to produce reasonable models for large scale electrolysis. To this end, we planned to investigate the electrolysis in a variety of melts, carry out lifetime measurements on the

electrode materials and perform ex-situ capture and analysis of the gas produced at the anode.

Experimental

Furnace Configuration

The electrolysis experiments were carried out in a 6 inch Mellen crucible furnace with MoSi_2 heating elements (Model: MT18-6X12-1Z). The unit consisted of two 99.8 % Al_2O_3 furnace tubes: a 24 inch high flat bottomed tube with a 5.5 inch outer diameter (OD) and a 24 inch high round bottomed 4.5 inch OD inner tube, to which the custom-designed furnace cap was attached. The tubes were stacked inside each other with Al_2O_3 beads (Zircar) between to allow even heat distribution to the electrochemical cell and to protect the furnace in case of crucible breakage. There were two 99.8% Al_2O_3 crucibles within the furnace tubes. A 3.3 inch OD inner crucible contained the electrolyte and electrodes and a 3.8 inch OD outer crucible acted as a containment crucible in case of breakage. The temperature of the furnace was controlled by the furnace heating unit (Mellen) attached to a type B thermocouple. The flow rate of the gases to and from the furnace was controlled by a mass flow controller and confirmed by a bubble meter. The oxygen concentration of the furnace exit gas was monitored with a Varian 4900 gas chromatograph.

Electrochemistry

For the melt characterization experiments, there were 3 working electrodes in the cells that were prepared from 1 mm diameter metal wires (Pt, Ir or Rh) immersed up to 2 cm in the electrolyte. These metal rods were attached to the 0.368 mm diameter Pt lead wire within mullite or alumina tubes. The counter electrode and reference electrode were both molybdenum rods (0.125" diameter) with mullite or alumina tubes to both insulate the electrode and shroud the molybdenum, such that only a small portion (1-3 cm) was exposed to the melt and none to the atmosphere above the melt.

For the larger scale experiments with oxygen detection, there were either two or three electrodes (WE, CE and an optional RE). The electrochemical cell was controlled by either a Solartron 1286 (running Corrware software) or PARSTAT 1273 (running Power Suite) potentiostat.

Electrolyte

The electrolyte was a 200 g oxide mixture selected to mimic the composition of lunar regolith. One melt was prepared from JSC-1a (Johnson Space Center-1a), a lunar simulant provided by NASA that was excavated from terrestrial sources, but has a similar composition and morphology to that of lunar regolith. The major difference between the electrolytes tested was the presence of Fe^{3+} , which is not present in lunar regolith, since all iron exists in the lower oxidation state of Fe^{2+} . The other selected melts (JSC-syn and JSC-syn with Fe^{2+}) were prepared from the appropriate oxide powders purchased from Aldrich and Alfa Aesar. These melts have no or limited transition metal oxides in their formulation. In the oxygen capture experiments, NaO was not added since it forms a gaseous Na product upon reduction, which reacts with any O_2 present.

Results and Discussion

Comparison of Melt Composition

Figure 1 compares the electrochemical characteristics of several melt compositions. By considering all possible theoretical, temperature corrected, redox potentials of the species present and by running melts of differing composition, it was possible to assign these electrochemical responses to the most likely reactions.

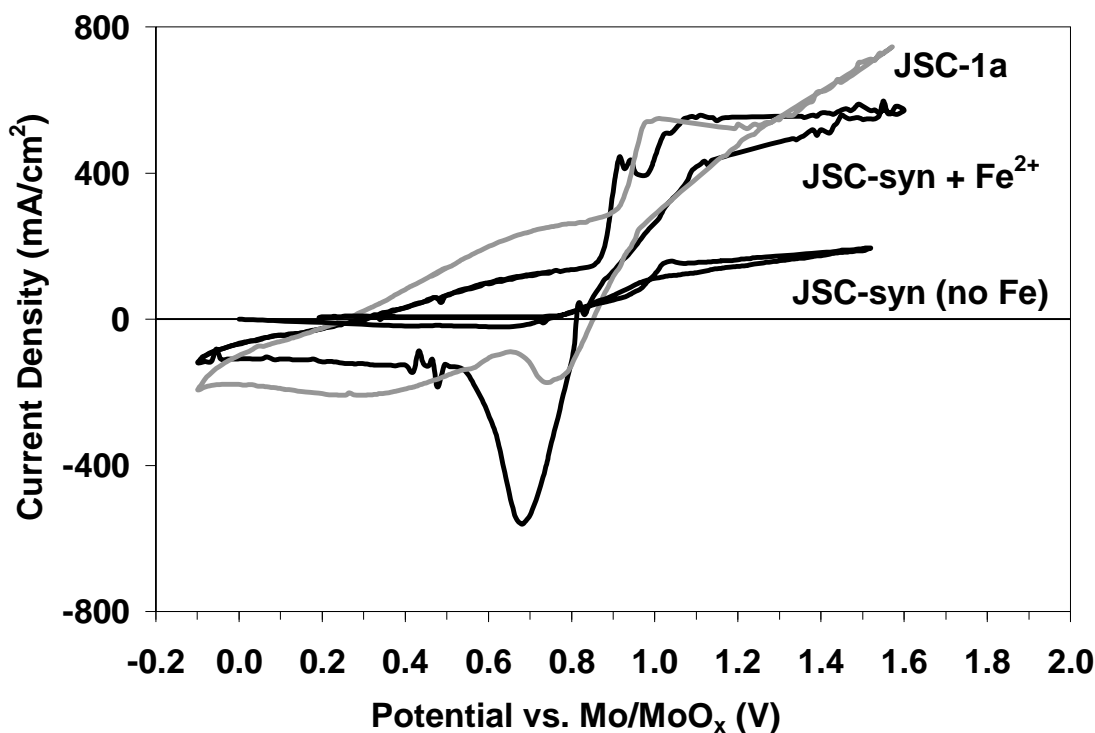


Figure 1. Cyclic voltammograms of Ir wire in three different melt compositions at 1575 °C; Mo counter electrode, Mo/MoO_x reference electrode, current-interrupt IR compensation, 100 mV s⁻¹.

For the iron-free melt (with neither Fe²⁺ nor Fe³⁺ present), as Ir electrode potential was scanned in an anodic direction from OCP (ca. 300 mV vs. Mo/MoO_x), minimal current was passed until potentials > 0.75 V (vs. Mo/MoO_x), at which the onset of oxide formation and concomitant oxygen evolution was detected. On the subsequent cathodic sweep, reduction of the adsorbed oxide or oxygen at the surface of the electrode occurred, followed by the possible reduction of sodium ions at potentials < 0.5 V (vs. Mo/MoO_x).

When Fe²⁺ was present, the melt composition most closely resembled that found on the lunar surface. Two competing anode reactions then occurred: the desired oxidation of oxides to form oxygen and the undesired oxidation of Fe²⁺ to produce Fe³⁺:



Unless the anode and cathode compartments are separated, oxidation of Fe^{2+} will lead to an unavoidable loss in current efficiency for oxygen production by reaction [1]. While separating anodic and cathodic compartments is simple with aqueous electrolyte solutions, materials compatibility challenges make this much more difficult to achieve in the presence of aggressive oxide melts. Combined with a higher concentration of free O^{2-} ions, which resulted from the slightly higher optical basicity (6), a higher anodic current was measured for this melt than for the corresponding iron-free melt. When the lunar simulant was investigated and Fe^{3+} was also present, additional current arose from electronic conductivity in the melt, due to the presence of both Fe^{2+} and Fe^{3+} in the melt and associated polaron hopping (7).

The oxidation current observed in the iron-free melt was confidently ascribed to the formation by reaction [1] of the desired product: oxygen gas. The presence of iron and other transition metal species in the other melts led to more complicated electrochemical signatures, but it was still possible to deduce reasonable redox processes responsible for the cyclic voltammetric behavior.

The characterization of the melts served a dual purpose. Not only did it give insight into the mechanism of the reaction, but it also mimicked the actual melt composition that will be observed in batch electrolyses, during which electrolyte compositions will change with time. The physical properties of the melt, such as density, viscosity, conductivity, heat capacity and melting point will also be changed significantly. The exact melt chemistry at any given time will be dependent on the feedstock (8), the extent of electrolysis and the feeding and withdrawal regimen of the cell.

Electrolysis in Lunar Simulant

While actual lunar regolith has only Fe^{2+} present, due to the absence of oxygen gas on the moon, the official lunar simulant (JSC-1a) provided by NASA is mined from terrestrial surfaces, so a mix of Fe^{2+} and Fe^{3+} is present in the resulting melt. This composition results in electrochemical behavior with multiple redox signals. By examining this melt at multiple scan rates, the specific reactions occurring can be investigated more closely. Figure 2 shows that oxidation currents, assigned to the oxidation of Fe^{2+} ions, increased at potentials > 0.2 V (vs. Mo/MoO_x); the current peak at 0.8-1.0 V (vs. Mo/MoO_x) was assigned to oxidation of Ir to Ir oxides, during which concomitant formation of O₂ gas occurred by reaction [1]. At potential sweep rates > 100 mV s⁻¹, diffusion-controlled currents were detected due to reaction [1] and [2] being limited by diffusion of both Fe^{2+} and O^{2-} ions. On the subsequent cathodic sweep, the current resulted from the reduction of Ir oxide, O₂ gas and Fe^{3+} ions. Due to the presence of both Fe^{2+} and Fe^{3+} , additional current was passed, owing to increased electronic conductivity of the melt.

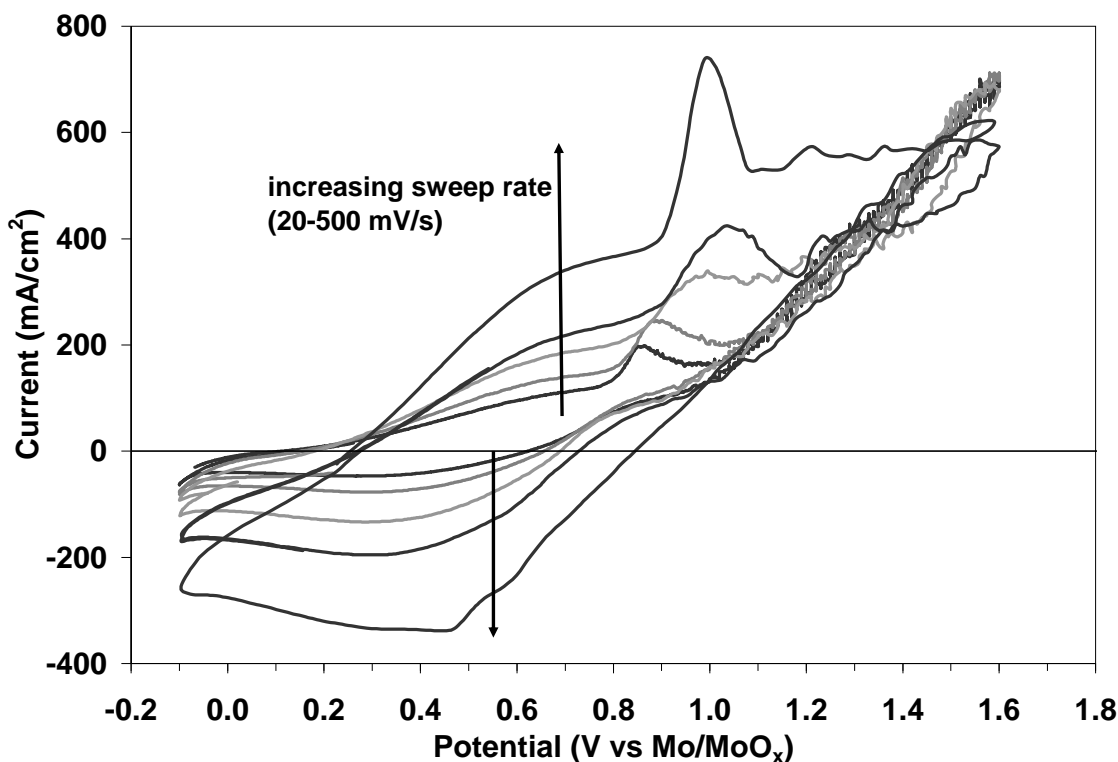


Figure 2. Effect of sweep rate on cyclic voltammograms of Ir in JSC-1a melt. Furnace temp of 1675 °C (melt temp 1575°C); Ir wire working electrode, Mo counter electrode, Mo/MoO_x reference electrode, current-interrupt IR compensation (20 mV s⁻¹, 50 mV s⁻¹, 100 mV s⁻¹, 200 mV s⁻¹, 500 mV s⁻¹).

Oxygen Analysis Experiments

A gas chromatograph was used to determine quantities of oxygen produced, enabling calculation of current efficiencies for reaction [1], and to confirm the proposed assignment of reactions in the cyclic voltammetric experiments. Therefore, instead of thin wires, larger electrodes were used with rods, foils, discs and open cubes, resulting in larger currents, so larger volumes of O₂ were produced. In some cases, the anode was encased in an anode collection tube to obtain a higher concentration of O₂. Continuous monitoring of the electrogenerated oxygen was carried out on exhaust gas from the furnace, enabling real-time measurements of current efficiencies for anode reaction [1].

Figure 3 shows a voltage profile and associated oxygen concentration profile for a typical run. As expected from the cyclic voltammograms, the oxygen concentration in the exit gas was zero at potentials < 0.8 V (vs. Mo/MoO_x), whereas at > 0.8 V, O₂ concentrations varied with melt chemistry, current and purge gas flow rate. In Figure 3, an increase in the concentration of oxygen over time was observed, as the concentration of electrogenerated oxygen in the exit gas reached steady state.

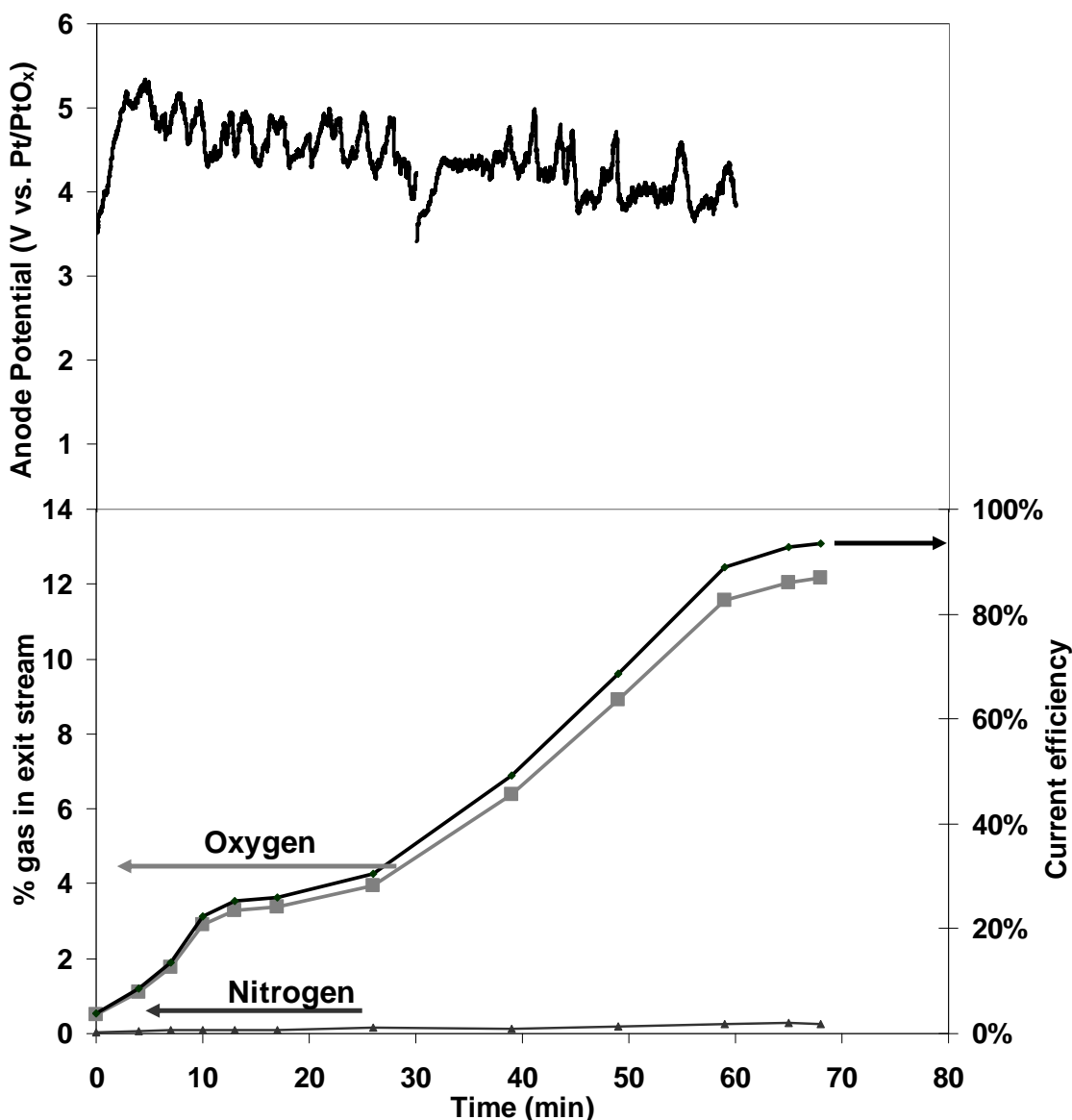


Figure 3. Electrolysis of iron-free molten oxide. Oxygen was collected using an anode containment tube; 0.2 Amp, Ir wire anode, Mo rod cathode and a Pt wire reference electrode.

Multiple experiments in the iron-free oxide melts at varying current densities resulted in current efficiencies for oxygen evolution ranging from 60 – 100%. The highest current efficiencies were measured when an anode collection tube was used, which collected the oxygen gas very effectively and isolated it from any other reactive components, but limited the size of the anode and therefore the total current passed. Several high temperature reactions of oxygen with the furnace components (Mo metal, carbon in the packing beads) were possible, which would have decreased current efficiencies. Moreover, the oxygen gas could move through diffusion or convection and be reduced at the cathode. When Fe^{2+} was present in the melt, current efficiencies decreased to a maximum of 60%, due to the parasitic oxidation of Fe^{2+} and the increased electrical conductivity of the melt with both Fe^{2+} and anodically-formed Fe^{3+} present.

Considerations for Scale-Up

Throughout these experiments, there were two main challenges: (a) reaction of electrogenerated oxygen with the furnace and cell components, and (b) melt containment. However, upon full scale-up, melt containment should not be an issue, since the cell would be self heating through excess joule heating that can be controlled by adjusting the inter-electrode gap, and since the containment would be formed from solidified regolith in a cold-walled configuration, as opposed to the present hot-walled vessel. Parasitic reaction of oxygen would also be limited at larger scale, as continued operation would eventually oxidize all reactive components.

Conclusions

The current responses in the cyclic voltammograms of an Ir electrode in a series of oxide melts at 1575 °C were assigned by changing the melt composition. These were verified by subsequent experiments with larger electrodes at constant current by analyzing oxygen concentrations in the off-gas by gas chromatography. Current efficiencies of 60 – 100% were measured in the iron-free melt. Reduced efficiencies of 30 – 60% were observed in the iron-containing melt, due to competing oxidation of Fe²⁺ to Fe³⁺ and increased electronic conductivity.

References

1. R. Aiken, Process of Making Iron From the Ore, US Patent 159609 (1903).
2. M. J. Oppenheim, *Min. Mag. and J. Mineral. Soc.*, **37**, 1104 (1968).
3. D. R. Sadoway, *JOM-J. Miner. Met. Mater. Soc.*, **43**, 15 (1991).
4. R. O. Colson and L. A. Haskin, in *Space 90, Engineering, Construction, and Operations in Space II*, S. Johnson and J. Wetzel (Eds.), p. 187 AIAA-ASCE New York (1990)
5. L. A. Haskin, R. O. Colson, D. J. Lindstrom, R. H. Lewis and K. W. Semkow, in *Lunar Bases and Space Activities of the 21st Century II*, p. 411, Lunar Bases and Space Activities of the 21st Century II, NASA Conf. Publ. 3166, Houston (1992).
6. A. Gmitter, Master's Thesis, Massachusetts Institute of Technology (2007).
7. M. Barati and K. Coley, *Metall Mater Trans B*, **37**, 41 (2006).
8. G. H. Heiken, D. T. Vaniman and B. M. French, *Lunar Sourcebook a User's Guide to the Moon*, Cambridge University Press, Cambridge (1991).